# List of Posters Presented

Srinandan C. S, Sarita Keni and Anuradha S. Nerurkar. 2006. Effect of divalent cations, pH and phosphate concentrations on biofilm formation at 3rd Convention of Biotech Research Society of India (BRSI) and International conference on "Exploring horizons in biotechnology: A global venture" from November 2-4 at SP University, VV nagar, Gujarat

Srinandan C .S, Samay Pande and Anuradha S. Nerurkar. 2007. Nitrate reduction efficiency and high nitrate tolerance studies of the denitrifying isolates *Acidovorax* sp.D1 and *Paracoccus* sp.W1b at National conference on " Current trends in Biochemistry" from December 27-29 at Nagpur University, Nagpur

Srinandan C. S, Vipul Jadav, Samatha Sripada and Anuradha S. Nerurkar. 2008. "Media components influencing *Paracoccus* sp.W1b biofilm structure, at 49th annual conference of Association of Microbiologists of India from 18-20 November, University of Delhi, Delhi

Srinandan C. S, Mrinal Shah, Bhavita Patel and Anuradha S. Nerurkar . 2009. Abundance and diversity of denitrifying bacteria in activated sludge, at 50th annual conference of Association of Microbiologists of India from 15-18 December, National Chemical Laboratory (NCL), Pune

Srinandan C. S and Anuradha S. Nerurkar. 2010. "Ca^{++} and Mg^{++} - induced biofilm differs architecturally in *Paracoccus* sp." at 'Biofilm 4' International conference, 1-3 September, 2010. Winchester, UK. (The poster was presented by Dr. A S. Nerurkar)

Srinandan C. S, Glen D'souza, B B. Nayak and Anuradha S. Nerurkar. 2010. on "Influence of different carbon sources and high nitrate on biofilm community structure in denitrifying conditions" at 51st annual conference of Association of Microbiologists of India, from 14-17 December 2010, Birla Institute of Technology, Mesra, Ranchi, Jharkhand
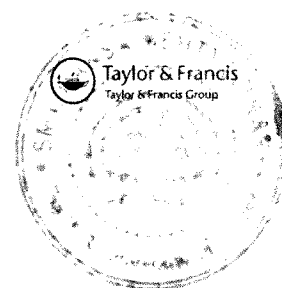
Nutrients determine the spatial architecture of *Paracoccus* sp. biofilm

C.S. Srinandan[a], Vipul Jadav[a], D. Cecilia[b] and A.S. Nerurkar[a]*

[a]*Department of Microbiology and Biotechnology Centre, Faculty of Science, M. S. University of Baroda, Vadodara, Gujarat, India;*
[b]*National Institute of Virology, Pune, India*

Bacterial biofilms adapt and shape their structure in response to varied environmental conditions. A statistical methodology was adopted in this study to empirically investigate the influence of nutrients on biofilm structural parameters deduced from confocal scanning laser microscope images of *Paracoccus* sp.W1b, a denitrifying bacterium. High concentrations of succinate, Mg^{++}, Ca^{++}, and Mn^{++} were shown to enhance biofilm formation whereas higher concentration of iron decreased biofilm formation. Biofilm formed at high succinate was uneven with high surface to biovolume ratio. Higher Mg^{++} or Ca^{++} concentrations induced cohesion of biofilm cells, but contrasting biofilm architectures were detected. Biofilm with subpopulation of pillar-like protruding cells was distributed on a mosaic form of monolayer cells in medium with 10 mM Mg^{++}. 10 mM Ca^{++} induced a dense confluent biofilm. Denitrification activity was significantly increased in the Mg^{++}- and Ca^{++}-induced biofilms. Chelator treatment of various biofilm ages indicated that divalent cations are important in the initial stages of biofilm formation.

Keywords: biofilm architecture; denitrification; image analysis; statistical design of experiment; divalent cations

Introduction

Biofilms are defined as matrix-enclosed bacterial populations adherent to each other and/or to surfaces (Costerton et al. 1995). Development of biofilm proceeds *via* the formation of (a) a monolayer (Moorthy and Watnick 2004), (b) microcolonies, (c) a mature biofilm, and (d) dispersal, where some biofilm cells revert to the planktonic lifestyle (Hall-Stoodley et al. 2004). Mature biofilms form complex architecture consisting of highly structured and well differentiated cells (Stoodley et al. 2002; Boles et al. 2004; Klausen et al. 2006; Vlamikis et al. 2008), which is also metaphorically called as 'city of microbes' (Watnick and Kolter 2000).

O'Toole et al. (2000) provided a conceptual framework for biofilm formation as a microbial development. However, Klausen et al. (2006) proposed that ecological adaptation of individual cells drives the evolution of biofilm spatial structure. Certain nutritional factors are known to influence biofilm development (Geesey et al. 2000; Prakash et al. 2003; Sauer et al. 2004; Song and Leff 2006; Monds et al. 2007; Schlag et al. 2007; Yang et al. 2007). The impact of nutrient composition on the architecture and physiochemistry of a degradative biofilm community has also been reported by Moller et al. (1997). In order to exploit full potential of biofilms in wastewater treatment, it is necessary to understand the influence of various environmental factors on biofilm structure, and in turn their activity.

In the present study, *Paracoccus* sp.W1b, a bacterium isolated from the denitrifying reactor sludge of a fertilizer company was used. The genus *Paracoccus* comprises metabolically versatile Gram-negative coccoid bacteria having the apparatus to denitrify nitrogenous oxides under anoxic conditions (Baker et al. 1998). Some *Paracoccus* species are also known to have attributes of degrading xenobiotics (Urakami et al. 1990; Siller et al. 1996; Vasilyeva et al. 2003; Peng et al. 2008; Xu et al. 2008). Their degradative abilities toward nitrate and other xenobiotics make them potential organisms for bioremediation. The isolate *Paracoccus* sp. W1b (hereafter *Paracoccus*) was found to have the ability to form biofilm and reduce high nitrate concentrations.

The Plackett–Burman statistical design of experiment approach was adopted to investigate the effect of seven different nutrient components on the *Paracoccus* biofilm in this study. Screening of nutrients by one-factor-at-a-time is time consuming, while a statistical approach helps to study the effect of several nutrient factors simultaneously. Plackett–Burman is a two level fractional factorial design in which each factor is tested an equal number of times at its high and low values and the influence of various factors can be determined

in a small number of trials (Plackett and Burman 1946). As such, the use of statistical designs for optimizing nutritional conditions to maximize yield is an established practice in industrial fermentation (Srinivas et al. 1994; Gohel et al. 2006; Akolkar et al. 2008).

With the hypothesis that nutrients influence the architecture of biofilms, the objective for this study was to investigate empirically the modulation of the architecture of the Paracoccus biofilm in response to nutrient concentrations using a statistical methodology. It is further reported here that the biofilms formed by Paracoccus in the presence of high Ca^{++} and Mg^{++} concentrations have different architectures and their structure is correlated with denitrification activity.

Materials and methods

Bacterial strain and culture conditions

A denitrifying isolate identified in the authors' laboratory as Paracoccus sp. was used in this study. The culture was maintained and an inoculum prepared in peptone nitrate medium (PNB). A 24 h old culture was centrifuged, washed and resuspended in phosphate buffered saline (PBS) before inoculation. Biofilm experiments were performed in MM2 medium consisting of sodium succinate 7.9 g, $MgSO_4.7H_2O$ 0.2 g, K_2HPO_4 0.2 g, $FeSO_4.7H_2O$ 0.05 g, $CaCl_2.2H_2O$ 0.02 g, $MnCl_2.4H_2O$ 0.002 g, $NaMoO_4.2H_2O$ 0.001 g, KNO_3 1.0 g, yeast extract 1.0 g, pH 7.0, distilled water 1000 ml. All experiments were performed at 30°C under static and anoxic conditions.

Plackett–Burman statistical design to screen nutrient components influencing biofilm

The Plackett–Burman design was used according to Montgomery (1997). MM2 was used as a basal medium and a total of seven medium components were selected for the study with each component/

variable being represented at two levels, high (+) and low (−) in 12 different media as shown in Tables 1 and 2. Nutrient concentrations were selected based on single parametric studies on biofilm formation in Paracoccus in the authors' laboratory. Each column in Table 1 represents a medium, and each row represents an independent/assigned or dummy/ unassigned variable with an equal number of positive and negative signs. The effect of each variable was determined by:

$$E(Xi) = \frac{2(\sum Mi^+ - \sum Mi^-)}{N} \quad (1)$$

where, $E(Xi)$ is the concentration effect of the tested variable. Mi^+ and Mi^- are the biofilm intensities or structural parameters in the medium where the variable (Xi) measured was present at high and low concentrations respectively, and N is the number of media. The experimental error was estimated by calculating the variance among the unassigned variables as follows:

$$V_{eff} = \frac{\sum(Ed)^2}{n} \quad (2)$$

where, V_{eff} is the variance of the concentration effect, Ed is the concentration effect for the unassigned variable and n is the number of unassigned variables. The standard error (SE) of the concentration effect is the square root of the variance of an effect.

$$SE = \text{Square root of } V_{eff} \quad (3)$$

The significance level (p value) of each concentration effect was determined by the Student's t test:

$$t(Xi) = \frac{E(Xi)}{SE} \quad (4)$$

where, $E(Xi)$ is the effect of variable Xi.

Table 1. Plackett–Burman design matrix

Variables/medium	A	B	C	D	E	F	G	H	I	J	K	L
X1	1	−1	1	−1	−1	−1	1	1	1	−1	1	−1
X2	1	1	−1	1	−1	−1	−1	1	1	1	−1	−1
X3	−1	1	1	−1	1	−1	−1	−1	1	1	1	−1
X4	1	−1	1	1	−1	1	−1	−1	−1	1	1	−1
X5	1	1	−1	1	1	−1	1	−1	−1	−1	1	−1
X6	1	1	1	−1	1	1	−1	1	−1	−1	−1	−1
X7	−1	1	1	1	−1	1	1	−1	1	−1	−1	−1
D1	−1	−1	1	1	1	−1	1	1	−1	1	−1	−1
D2	−1	−1	−1	1	1	1	−1	1	1	−1	1	−1
D3	1	−1	−1	−1	1	1	1	−1	1	1	−1	−1
D4	−1	1	−1	−1	−1	1	1	1	−1	1	1	−1

X, Assigned variables; D, Unassigned variables.

Table 2. Variables with media components and their concentrations.

Variables	Components	+ values (mM)	− values (mM)
X1	KNO_3	100.0	0.1
X2	Succinate	50.0	0.5
X3	$MgSO_4$	15.0	0.15
X4	$FeSO_4$	1.0	0.1
X5	K_2HPO_4	10.0	0.01
X6	$CaCl_2$	15.0	0.15
X7	$MnCl_2$	1.0	0.01

Microtiter plate assay for biofilm quantification

Biofilm formation was assayed by measuring the bacterial biomass adhered to microtiter wells. One milliliter of MM2 medium was inoculated with 10^8 cells in a 24-well polystyrene microtiter plate. After the incubation period, the wells were rinsed five times with 1.5 ml of sterile PBS to remove any adhering planktonic cells. The biofilm was then stained with 1.5 ml of 1% crystal violet for 45 min, rinsed five times with 1.5 ml of water and destained with 70% ethanol for 15 min. Absorbance of the solution was measured at 595 nm.

Confocal microscopy and image analysis

Polystyrene slides with 2 cm × 2 cm diameter were used for biofilm formation and these were incubated in Petri dishes containing medium at 30°C for 24 h under static conditions. The slides were then rinsed with sterile PBS (pH 7.4) and stained with LIVE/DEAD baclight® (Invitrogen) according to manufacturer's instructions. Image acquisition was done at 40 × with a Zeiss (LSM 510 Meta) confocal laser scanning microscope (CSLM). Two to four independent slides and three to seven fields from each slide were randomly chosen to acquire images with constant microscopic settings; overall 245 images were processed. Raw images were processed by IMARIS and Adobe Photoshop softwares. Quantification of biofilm parameters was done by a COMSTAT program written as a script in MATLAB 5.1 (Heydorn et al. 2000). Live to dead ratios were calculated by measuring densities of red and green fluorescence images by ImageJ, a NIH freeware (http://rsb.info.nih.gov/ij/index.html).

Environmental scanning electron microscopy

Biofilm formed on polystyrene slides were treated according to Priester et al. (2007) with a few modifications. Slides were stained with 0.05% ruthenium red and 2.5% glutaraldehyde (used as a fixative) in 0.1 M HEPES buffer (pH 7.3, Sigma chemicals) for

30 min. Further, the slides were washed with HEPES buffer, dried, and observed under an ESEM (XL-30, Philips, Netherlands).

Biofilm experiments with chelator treatment

The effect of ethylenediaminetetraacetic acid (EDTA) on biofilm formation was assessed by adding 0.0–10.0 mM EDTA in MM2 medium and biofilm formation was assayed by the microtiter plate technique.

To investigate the influence of chelators on biofilms of various ages, the following procedure was followed. Biofilm was grown in Petri dishes containing polystyrene slides in either MM2, MM2-Ca (MM2 medium containing 10 mM $CaCl_2$) or MM2-Mg (MM2 medium containing 10mM $MgSO_4$). Biofilm slides 6, 12, 18, and 30 h old were rinsed with PBS and treated with 10 mM EDTA (for MM2 or MM2-Mg grown biofilms) or ethylene glycol tetraacetic acid (EGTA) (for MM2-Ca grown biofilm) for 30 min. Control biofilms were treated with PBS. The biofilm was stained with LIVE/DEAD baclight for confocal microscopy and biomass was measured by COMSTAT. The percentage of biomass reduced by chelator treatment was calculated by the following equation:

$$\frac{(B1 - B2)100}{B1} \tag{5}$$

where, B1 = the average biomass in PBS treated biofilm, B2 = the average biomass in chelator treated biofilm

Analytical methods

The brucine sulfate method was used to determine nitrate according to Jenkins and Medsker (1964). Nitrite was estimated according to APHA (1995). Lowry's method was used to determine protein concentrations (Lowry et al. 1951).

Results

Nutrients influence biofilm formation

The biomass in terms of the intensity of the eluted crystal violet from microtiter plates was used as the measure of biofilm formation. Results of the Plackett–Burman experiment for the effect of nutrients on biofilm formation, as shown in Figure 1a indicate that medium B produced high biofilm, followed by media F and H. The effects of different components on biofilm formation and planktonic growth were further interpreted by calculating the $(E(Xi))$ values and Figure 1b represents $E(Xi)$ values calculated for biofilm
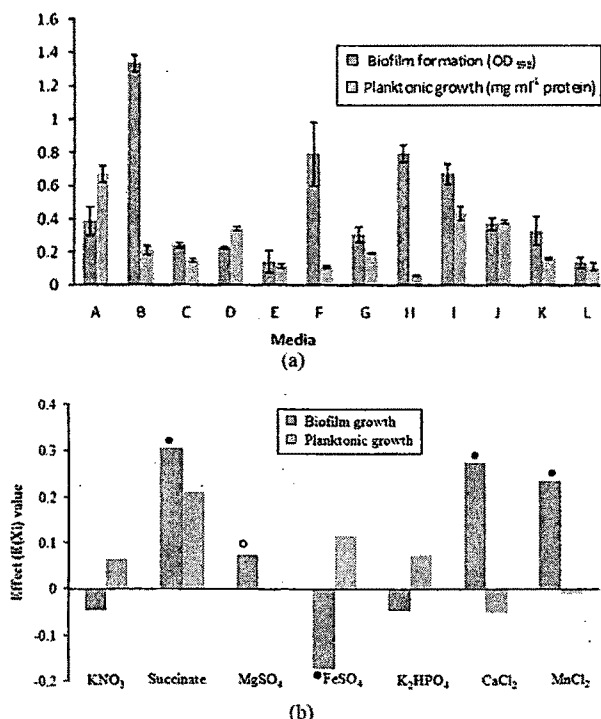
Figure 1. Nutrient components influencing *Paracoccus* biofilm formation. (a) Biofilm formation and planktonic growth in different media of Plackett–Burman experiment. Bars represent average values of three independent experiments. Error bars represent SDs. (b) Effect $(E(Xi))$ values of the nutrient components on biofilm formation and planktonic growth. ● Significant at $p < 0.05$; ○ significant at $p < 0.1$.

Figure 2. Representative CSLM images (40 × magnification) of *Paracoccus* biofilm structures formed in the 12 different media A–L of the Plackett–Burman experiment.

formation. A positive $E(Xi)$ value of the variable is considered to induce biofilm formation at the higher concentration tested, and when negative, the variable is considered to induce biofilm formation at lower concentrations. Succinate, $MgSO_4$, $CaCl_2$, and $MnCl_2$ showed positive $E(Xi)$ values ($p \leq 0.1$), thus significantly inducing biofilm formation at higher concentrations. $FeSO_4$ showed a negative $E(Xi)$ value ($p \leq 0.05$) inducing biofilm formation at lower concentrations. Succinate showed a nearly significant ($p = 0.112$) positive influence on planktonic growth.

Nutrients modulate biofilm architecture

The effect of nutrients on biofilm architecture was analyzed by studying their influence on six different biofilm structural parameters deduced from CSLM images (Figure 2a–l). The results of biofilm quantification for 12 different media of Plackett–Burman design are given in Table 3. Medium C produced high biomass, average thickness, substratum coverage and a low roughness coefficient, implying formation of a
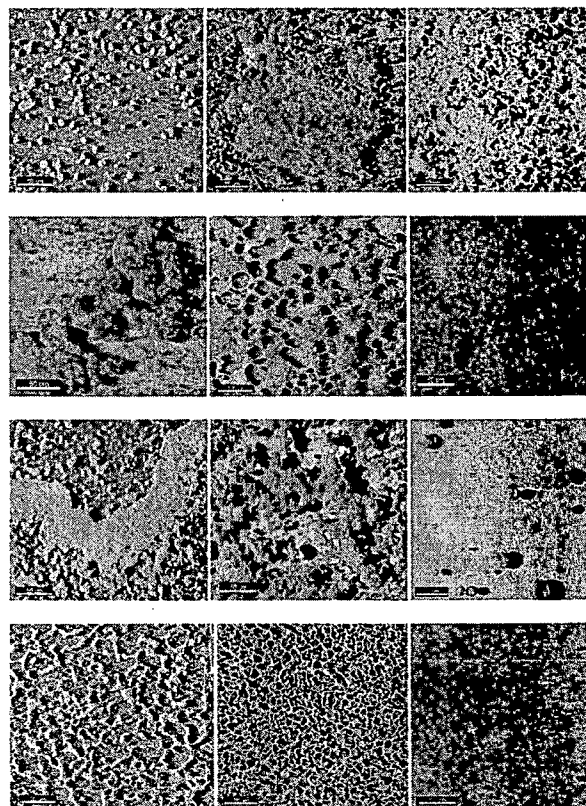
thick and homogenous biofilm. Media A and F showed decreased biomass, average thickness, maximum thickness and substratum coverage and high values of roughness coefficient and surface to biovolume ratio, entailing the formation of an uneven flat biofilm.

Table 4 shows the effect $(E(Xi))$ and the corresponding p values of seven different nutrient components on the six biofilm parameters. The positive $E(Xi)$ value means that the particular medium component induced a corresponding biofilm parameter at its higher concentration and a negative value implies a lower concentration of the medium component has a positive effect on the biofilm parameter. If the surface to biovolume ratio is affected positively, it means that a high fraction of cells in the biofilm were exposed to the bulk liquid and a negative effect implies that the fraction of cells exposed to bulk liquid was low.

Succinate affected biomass negatively ($p < 0.05$) whereas the maximum thickness ($p < 0.05$), roughness coefficient ($p < 0.1$), and surface to biovolume ratio ($p < 0.1$) reacted positively. This indicates that the biofilm formed at high succinate concentrations were

Table 3. Structural parameters of biofilm formed in twelve different media of the Plackett–Burman experiment quantified from the CSLM images.

Medium	A	B	C	D	E	F	G	H	I	J	K	L
Biomass ($\mu m^{-3}\,\mu m^{-2}$)	0.02 ± 0.001	3.47 ± 0.38	12.17 ± 0.78	0.51 ± 0.38	6.73 ± 1.03	0.02 ± 0.0005	5.60 ± 2.30	3.34 ± 0.94	2.29 ± 0.07	2.07 ± 1.33	3.53 ± 0.26	3.45 ± 0.94
Average thickness (μm)	0.01 ± 0.003	15.86 ± 2.18	38.47 ± 2.70	4.74 ± 3.76	16.47 ± 0.87	0.006 ± 0.001	13.44 ± 5.69	17.21 ± 7.36	19.60 ± 1.74	4.87 ± 0.60	10.25 ± 1.30	22.47 ± 12.22
Roughness coefficient	1.86 ± 0.20	1.41 ± 0.66	0.09 ± 0.01	1.68 ± 0.26	0.56 ± 0.11	1.99 ± 00	0.36 ± 0.17	1.49 ± 0.63	0.77 ± 0.09	1.54 ± 0.51	0.41 ± 0.09	0.23 ± 0.18
Surface:bio-volume ($\mu m^{-2}\,\mu m^{-3}$)	6.26 ± 1.20	3.27 ± 0.26	4.45 ± 0.15	5.56 ± 1.23	2.67 ± 0.16	6.95 ± 0.01	3.63 ± 0.50	3.94 ± 0.74	4.26 ± 0.45	4.05 ± 0.57	3.70 ± 0.32	4.05 ± 0.58
Maximum thickness (μm)	28.50 ± 4.95	48.18 ± 5.80	44.53 ± 2.71	28.20 ± 2.89	33.10 ± 1.93	29.63 ± 2.26	22.05 ± 4.73	44.63 ± 4.53	59.22 ± 6.861	40.32 ± 12.47	17.08 ± 1.57	32.26 ± 13.40
Substratum coverage	0.02 ± 0.003	0.02 ± 0.002	0.20 ± 0.006	0.03 ± 0.007	0.05 ± 0.01	0.02 ± 0.0005	0.09 ± 0.05	0.03 ± 0.004	0.07 ± 0.03	0.07 ± 0.09	0.03 ± 0.006	0.11 ± 0.06

Table 4. Statistical analysis for influence of nutritional components on biofilm structural parameters from the results of Plackett–Burman design.

Variable	KNO_3 $E(Xi)$	p value	Sodium succinate $E(Xi)$	p value	$MgSO_4$ $E(Xi)$	p value	$FeSO_4$ $E(Xi)$	p value	K_2HPO_4 $E(Xi)$	p value	$CaCl_2$ $E(Xi)$	p value	$MnCl_2$ $E(Xi)$	p value
Biomass	1.78	0.1	−3.29	0.02	2.88	0.03	−1.09	0.26	−0.58	0.51	1.38	0.17	0.82	0.37
Average thickness	5.76	0.51	−6.46	0.47	7.93	0.38	−7.78	0.39	−6.97	0.44	2.1	0.8	3.47	0.68
Roughness coefficient	−0.4	0.33	0.85	0.09	−0.47	0.27	0.45	0.28	0.02	0.94	0.4	0.33	0.03	0.92
Surface:biovolume	−0.05	0.72	0.31	0.09	−1.33	0.002	1.52	0.001	−0.43	0.04	0.38	0.06	0.57	0.02
Maximum thickness	0.72	0.8	11.73	0.02	9.52	0.03	−8.53	0.04	−12.24	0.01	4.9	0.16	5.98	0.11
Substratum coverage	0.02	0.36	−0.04	0.11	0.02	0.29	−0.003	0.9	−0.04	0.11	−0.01	0.63	0.01	0.4

uneven in thickness with more cells exposed to the bulk liquid. Mg^{++} affected the biomass ($p < 0.05$) and maximum thickness ($p < 0.05$) positively and surface to biovolume ratio negatively ($p < 0.05$), suggesting that the cells were densely clustered. Nitrate affected the biomass positively ($p = 0.109$). Ca^{++} influenced surface to biovolume ratio, biomass, and maximum thickness positively, ($p = 0.06$, $p = 0.178$, and 0.162, respectively) implying that a thick biofilm was formed at high calcium levels with more cells exposed to the bulk liquid.

Ca^{++} and Mg^{++} affect the biofilm architecture differentially

Higher concentrations of Ca^{++} and Mg^{++} were observed to increase biofilm formation. The mechanism for biofilm enhancement by Ca^{++} and Mg^{++} is possibly by inducing cohesion, which was found to be so in the *Paracoccus* biofilm as visualized by ESEM images. Biofilm of aggregated cells with distinct voids and a dense mass of biofilm cells were observed in MM2 medium with 10 mM $MgSO_4$ (MM2-Mg) and

(a)   (b)   (c)

(d)   (e)   (f)
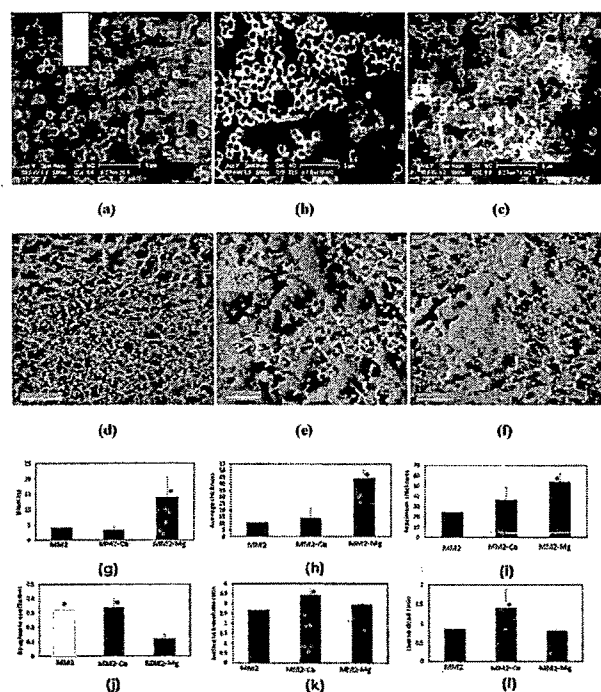
(g)   (h)   (i)

(j)   (k)   (l)

Figure 3. Comparison of *Paracoccus* biofilm structures formed in different media. (a–c) ESEM images of biofilm grown in MM2 medium, MM2-Mg, and MM2-Ca, respectively. CSLM images of biofilm (40 × magnification) formed in (d) MM2 medium (e) MM2-Mg (f) MM2-Ca (g–l). COMSTAT results of various biofilm parameters from the CSLM images. One way ANOVA with Tukey test was used to determine significant differences. • = significance $p < 0.05$.

10 mM $CaCl_2$ (MM2-Ca), respectively (Figure 3b and c). Biofilm in the control MM2 medium showed no such typical aggregations, although disconnected cells attached to the substratum were seen (Figure 3a). Clusters of cells were observed to be glued together in biofilms of high Ca^{++} and Mg^{++} suggesting induction of cohesion by these cations.

Further investigation of biofilms formed at high levels of Ca^{++} and Mg^{++} was done by analyzing their structures from CSLM images. Although Ca^{++} and Mg^{++} enhanced biofilm growth by the same mechanism of inducing cohesion as visualized in ESEM micrographs (Figure 3a–c), they affected surface to biovolume ratio differentially as observed from CSLM image analysis (Table 4). The $E(Xi)$ values of biomass and thickness were positive for both the cations, but the surface to volume ratio was negative in MM2-Mg ($p < 0.05$) and positive in MM2-Ca ($p = 0.06$) (Table 4), suggesting that the overall architecture was affected differentially. To validate this observation, biofilm was allowed to form in MM2-Mg, MM2-Ca, and control MM2 medium. MM2-grown biofilm showed a well networked mosaic structure with distinct voids (Figure 3d). Dense and confluent biofilm was observed in MM2-Ca (Figure 3f), whereas a monolayer of cells with a mosaic skeletal structure and dense protruding pillars of cells distributed over them was observed in MM2-Mg-grown biofilm (Figure 3e). Biomass, average thickness, maximum thickness, and substratum coverage was higher and the roughness coefficient significantly lower in the Mg^{++}-induced biofilm as shown in Figure 3g–k. In the Ca^{++}-induced biofilm, the surface to biovolume ratio and the roughness was significantly higher than in the biofilm grown in MM2-Mg medium (Figure 3g–k) validating the earlier observation. Though the divalent cations, Ca^{++} and Mg^{++} are thought to induce the biofilm in similar way by crosslinking the cells and matrix, the overall architecture was found to be distinctly different.

Ca^{++}- and Mg^{++}-induced biofilm demonstrate enhanced denitrification activity

Denitrification activity was measured for the biofilms formed in MM2-Mg or MM2-Ca medium to correlate biofilm structure with denitrifying activity. Figure 4 shows nitrate reduction was significantly higher in the Ca^{++}- and Mg^{++}-induced biofilm compared to biofilms grown in MM2 medium. It was 5.9 fold higher in MM2-Ca and 6.3 fold higher in MM2-Mg compared with MM2 biofilm. Significant difference was not observed in nitrate reduction or nitrite accumulation between biofilms formed in presence of high Ca^{++} and Mg^{++}.
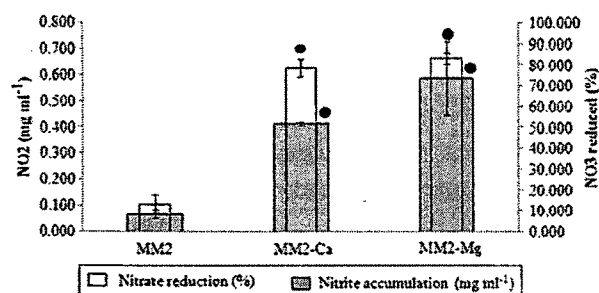
Figure 4. Denitrification activity (6 h incubation) of a *Paracoccus* biofilm grown in MM2, MM2-Mg, and MM2-Ca. Initial nitrate = 3 mM. Bars represent average values of at least three independent experiments and error bars represent the SDs. One way ANOVA with Tukey test was used to determine significant differences. ● = significance $p < 0.05$.
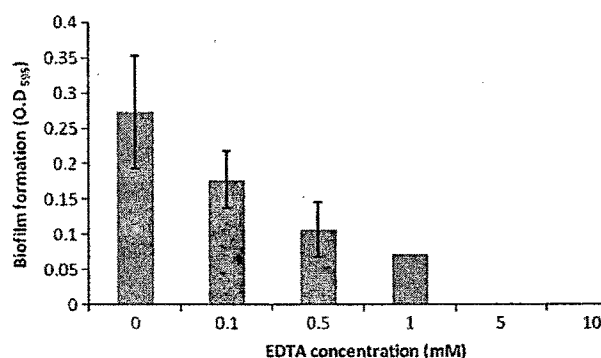

Figure 5. Effect of EDTA on *Paracoccus* biofilm formation.

Figure 6. Percentage of biomass reduction at various ages of *Paracoccus* biofilm by EDTA/EGTA treatment.

Chelator treatment reveals the importance of divalent cations in biofilm development

The role of divalent cations in biofilm formation by *Paracoccus* was further investigated by adding EDTA to the medium. An average of 1.56 fold reduction in biofilm formation was observed with every increase in EDTA concentration up to 0.5 mM (Figure 5). Biofilm formation was completely inhibited at 1.0 and 10 mM EDTA. Planktonic growth determined by the colony forming unit (CFU) count was found to be 10^{12} ml^{-1}, in media containing EDTA in the range 0.0–0.5 mM, but its toxic effect was observed at concentrations > 0.5 mM. CFU counts of 10^9, 10^6, and 10^5 ml^{-1} were obtained with EDTA concentrations of 1.0, 5.0, and 10 mM, respectively.

Though biofilm formation decreased at increasing EDTA concentration, complete inhibition was not found at non-toxic EDTA concentrations. Hence, various ages of biofilm grown in MM2, MM2-Mg and MM2-Ca were treated with 10 mM EDTA or EGTA. Biomass in MM2 medium showed a reduction of 62% and 79% at the 6 h and 12 h old stages, respectively after EDTA treatment and no reduction thereafter was observed, as shown in Figure 6. When Ca^{++}-induced biofilm of various ages was treated with 10 mM EGTA, a 99% decrease in biomass was observed at 6 h and an 82% reduction at 12 h. Like the control MM2, a further reduction was not found in biofilm with EGTA treatment at other time intervals, indicating that some divalent cations including Ca^{++} are significant in the initial stages of biofilm development possibly conferring structural stability by forming crosslinkages between cells or the matrix. Biofilm in 10 mM Mg^{++} showed reductions of biomass in the range 68–74%, although at 12 h it showed a 42% reduction. Pillar-like protruding cells of the biofilm were mainly found to detach after EDTA treatment in
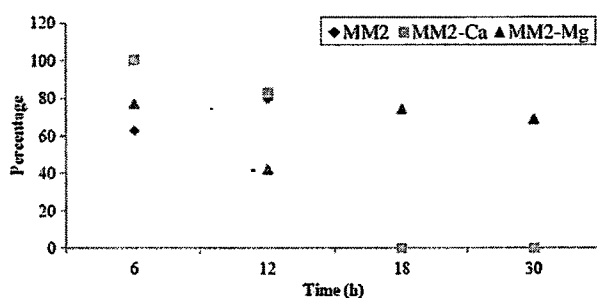
the high Mg^{++} medium after a 12 h period (Figure 7a and b).

Discussion

In order to investigate the influence of nutrients on biofilm formation by *Paracoccus*, a statistical design of experiment by microtiter plate assay was used. The assay utilized crystal violet staining, which binds to negatively charged molecules on the cell surface including EPS with acidic residues, thus quantifying the overall biomass which is the measure of biofilm formed. The influence of nutrient parameters on biofilm formation was observed to be distinct in 12 different media by either inducing or repressing biofilm formation. $E(Xi)$ values based on the assay showed significant increase in biofilm formation affected by succinate, Ca^{++}, Mg^{++}, and manganese, whereas iron repressed biofilm formation at higher concentrations.

Biofilm architecture, as affected by various nutrients, was determined by combining the different structural parameters quantified from confocal images. Fluorescent nucleic acid stains, ie, SYTO9 and propidium iodide were used to stain biofilm for confocal microscopy and the images were used to quantify the structural parameters including biomass by the COMSTAT program. All the nutrient
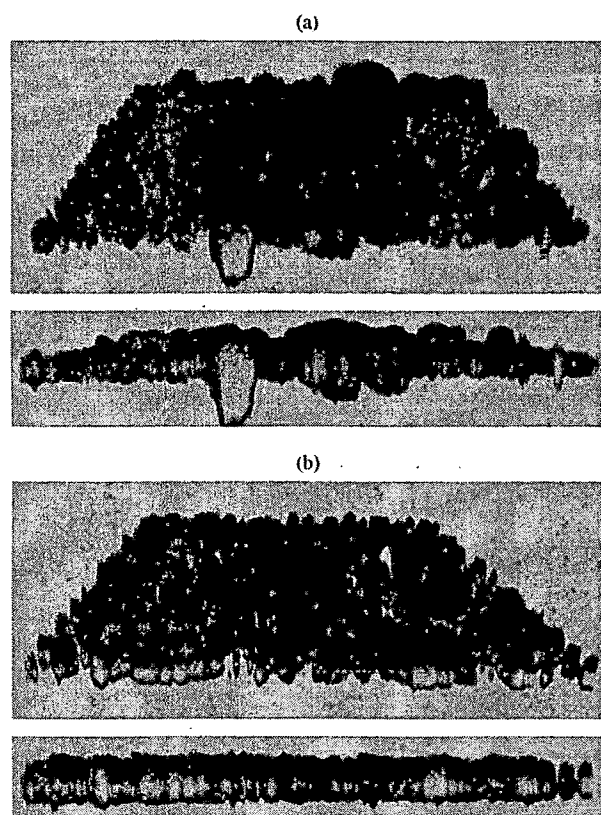
(a)

(b)

Figure 7. 3D image and its corresponding Z-projection of the 18 h old *Paracoccus* biofilm grown in MM2-Mg medium (a) before EDTA treatment; (b) after EDTA treatment.

components used were shown to significantly or nearly significantly affect every biofilm parameter tested, except average thickness, emphasizing the importance of their concentrations on modulating biofilm structures (Table 4). The adaptation of biofilm structure according to changes in local substrate concentrations has also been predicted by computational models (Wimpenny and Colasanti 1997).

High succinate concentrations affected biofilm formation positively as shown by the microtiter plate assay (Figure 1b) whereas image analysis showed a higher concentration of succinate to affect biomass negatively, but maximum thickness, the roughness coefficient, the surface to volume ratio, and the live to dead ratio positively (Table 4). The microtiter plate assay gives the intensity value of crystal violet as the overall biomass in the biofilm, whereas the COMSTAT analysis of the image reflects the amount of biomass (the fluorescent intensity of stained nucleic acids) excluding exopolysaccharides or proteins in the biofilm. The disparity between the microtiter plate and confocal image analysis is possibly due to the increased production of exopolysaccharides at higher

concentration of succinate. Enhanced synthesis of EPS due to the availability of an excess carbon source has also been discussed in a review on biofilm exopolysaccharides by Sutherland (2001).

Iron showed negative $E(Xi)$ values for biomass ($p = 0.26$) and maximum thickness ($p = 0.04$) implying a positive influence on these parameters at lower concentrations (Table 4). Planktonic growth was not significantly affected by higher iron concentrations (Figure 1b) indicating that the higher concentrations used were not toxic to growth. Reduction in biofilm formation at increasing iron concentrations has been reported for *Pseudomonas aeruginosa* (Musk et al. 2005; Yang et al. 2007) and *Staphylococcus epidermidis* strains (Johnson et al. 2005). Reduction in biofilm biomass and thickness at high levels of iron was also observed by Yang et al. (2007). However, the importance of minimal amounts of iron in biofilm development is demonstrated by Singh et al. (2002) and Banin et al. (2005). Deighton and Borland (1993) showed increased slime production in iron-limited conditions for *S. epidermidis* strains known to form biofilms encased with slime on prosthetic medical devices. Yang et al. (2007) observed a decrease in extracellular DNA with increasing iron concentrations and these authors also discussed their unpublished result where lower levels of iron induced increased production of extracellular DNA. This illustrates that lower levels of iron are necessary for biofilm formation, whereas excess iron represses biofilm formation.

Divalent cations other than iron, such as Ca^{++}, Mg^{++}, and manganese, showed a positive effect on biofilm formation in the microtiter plate assay and this was significant at higher concentrations (Figure 1b). Many reports have demonstrated the involvement of Ca^{++} in biofilm formation. Kierek and Watnick (2003) showed the important role of O-antigen in Ca^{++}-dependent biofilm formation in *Vibrio cholerae*. Addition of Ca^{++} enhanced biofilm thickness by nearly 20-fold in mucoid *P. aeruginosa* biofilms (Sarsikova et al. 2005). Mg^{++} is also known to enhance biofilm formation. Adhesion of *S. epidermidis* increased two to four fold with addition of Ca^{++} and Mg^{++} to plastic (Dunne and Burd 1992). Song and Leff (2006) observed an increase in bacterial attachment with increasing Mg^{++} concentrations. Statistical analyses of *Paracoccus* biofilm structures showed that Ca^{++} and Mg^{++} positively affected biomass and maximum thickness (Table 4). Tanji et al. (1999) showed that the thickness of biofilm increased due to an increase in the density of dead cells in the biofilm. Thus, the live to dead ratio of cells was also calculated in the present study, and a significant increase in the live cell fraction was found in biofilm grown in MM2-Ca medium and

no significant difference was observed between MM2 and the MM2-Mg grown biofilms (Figure 3l), suggesting that the accumulation of dead cells was not a reason for the increase in the thickness of the *Paracoccus* biofilm.

Chen and Stewart (2002) observed a reduction in the apparent viscosity of *P. aeruginosa* biofilm cells with Ca^{++} and Mg^{++}, whereas the viscosity increased with iron salts. Contrary to this observation, ESEM visualization of *Paracoccus* biofilm indicated cohesion of cells induced by Ca^{++} and Mg^{++} (Figure 3a–c), thus enhancing biofilm formation, whereas repression of biofilm formation was observed by iron at higher concentrations (Figure 1b and Table 4). However, in results provided by CSLM a contrast in structure was observed for the biofilm formed at high levels of Ca^{++} and Mg^{++}. Mg^{++} affected the surface to volume ratio negatively, whereas Ca^{++} affected it positively (Table 4). A negative surface to volume ratio implies a lesser fraction of cells exposed to bulk liquid. Increased biomass with a low surface to volume ratio indicates clustering of cells into tall pillars, which allows a lower fraction of the cells to be surface exposed, but the converse is true for a positive surface to volume ratio. Contrasting biofilm structures were formed, though both are thought to contribute to cohesion by cross-linking the cells and the matrix in the same way. Lattner et al. (2003) demonstrated differential affinity of Ca^{++} and Mg^{++} to alginate, a major EPS produced by *P. aeruginosa* biofilm. This disparity is possible because of the difference in their orbital structure, binding strength, and the rate constant of binding to the cell surface or matrix molecules (Geesey et al. 2000). Klausen et al. (2006) have proposed that the natural selection of different biofilm subpopulations in response to environmental conditions is the underlying reason for structural differences in *P. aeruginosa* biofilms grown in the presence of citrate or glucose. Similarly in this study with *Paracoccus*, a high level of Ca^{++} and Mg^{++} possibly promoted the formation of a protruding subpopulation of cells at different frequencies contributing to the difference in biofilm architecture.

Wimpenny and Colasanti (1997) reviewed three different conceptual models of biofilm structures, the water-channel, heterogenous mosaic, and a dense biofilm model. Comparisons can be drawn here to these models with *Paracoccus* biofilm. A typical mosaic form of biofilm cells with distinct voids was observed in the biofilm grown in control MM2 medium (Figure 3d), similar to the water-channel model. Some parallels between the Mg^{++}-induced biofilm with the heterogenous mosaic model and the Ca^{++}-induced biofilm with the dense biofilm model were also observed. The Mg^{++}-induced biofilm of *Paracoccus* showed pillar-like

protrusions of cell clusters distributed on a monolayer of a mosaic kind of networked cells (Figure 3e). In a heterogenous mosaic model, well separated stacks of microcolonies are attached to the substratum with a small bottom layer of cells in the background. This kind of biofilm structure was described for natural biofilm in water distribution systems. The Ca^{++}-induced biofilm of *Paracoccus* formed dense, confluent aggregations of cells (Figure 3f). Dental plaque biofilms comply with the dense biofilm model (Wimpenny and Colasanti 1997). Saliva-derived components are also been known to have a high level of Ca^{++} ions (Garcia-Godoy and Hicks 2008) and aggregation of cells induced by Ca^{++} in a cariogenic strain of *Streptococcus downei* has been demonstrated by Rose (2000).

Addition of EDTA to the medium decreased the amount of biofilm formation by *Paracoccus* (Figure 5) indicating the role of divalent cations in biofilm development. Turakhia et al. (1983) treated a biofilm with EGTA causing it to detach, signifying the role of Ca^{++} in clasping the cells together. Reduction in the adhesion of *S. epidermidis* cells by EDTA treatment was observed by Dunne and Burd (1992). A decrease in apparent viscosity on EDTA treatment (Chen and Stewart 2002) and loss of biofilm cells by addition of EDTA was also found in *P. aeruginosa* (Banin et al. 2006). Though there is a reduction, complete inhibition of biofilm formation was not observed in any of these studies. Hence, biofilms of various ages were treated with the chelator in this study to examine the role of divalent cations during biofilm development. Biofilm in MM2 and MM2-Ca media showed no reduction in biomass after a 12 h period with chelator treatment (Figure 6). This suggests that divalent cations are necessary in the initial stages of biofilm development. Nutrients such as phosphate and iron are also implicated in the microcolony and the maturation stages, respectively during biofilm development (Banin et al. 2005; Monds et al. 2007). On the other hand, increased biomass reduction with time was observed for the biofilm grown in MM2-Mg medium treated with EDTA (Figure 6). The availability of a higher Mg^{++} concentration was possibly exploited by a subpopulation of *Paracoccus* even at later stage of development, as a result of which they were susceptible to the EDTA treatment. It was also observed that the protruding pillar-like cells were more susceptible to EDTA than the basal mosaic layer of cells in the 10 mM Mg^{++} supplemented medium (Figure 7b), indicating that the pillar-like cells were held together possibly by Mg^{++} ions. This indicates that protruding cells are possibly subpopulations naturally selected by a high level of Mg^{++} unlike the basal mosaic layer.

High nitrate levels did not show a significant effect on biofilm formation as observed by microtiter plate

assay, although it had a positive influence on biomass ($p = 0.109$) as analyzed from CSLM images. Other biofilm parameters were not significantly influenced by altered nitrate levels. Nitrite, an intermediate of denitrification has been shown to inhibit *Staphylococcus aureus* biofilm formation (Schlag et al. 2007) and nitric oxide has been implicated in the dispersal of *P. aeruginosa* biofilm (Barraud et al. 2006). Activation of the denitrification pathway requires not only the presence of nitrate but also oxygen-limiting conditions (Tiedje 1994). Denitrification activity was significantly higher in the MM2-Ca and the MM2-Mg biofilm than in the MM2 biofilm of *Paracoccus*. Decreasing dissolved oxygen (DO) concentrations from the bulk fluid phase into the microcolony was observed in dense biofilms, but significant levels of DO were seen in less dense microcolonies by Costerton et al. (1995). Biofilm grown in MM2-Ca and MM2-Mg formed thick biofilms with high biomass compared to the biofilm grown in MM2 medium (Figure 3g–i), suggesting that the reduced DO concentration is the possible reason for inducing more denitrification activity. However, denitrification was not significantly different between MM2-Ca and MM2-Mg biofilms.

The statistical design of the present experiment demonstrated the modulated response of the *Paracoccus* biofilm architecture to varied nutrient concentrations. It would be interesting to develop such statistical designs for high thoroughput screening of environmental impacts on biofilm structure to activity for various applications, including monitoring of substrates qualitatively and quantitatively, to improve reactor efficiency in wastewater treatment processes. Biofilm development in *Paracoccus* was significantly affected by the divalent cations Ca^{++} and Mg^{++}, enhancing biomass and the thickness of the biofilm at higher concentrations which in turn affected denitrification. This could be exploited in nitrate removal processes to provide anoxic conditions for increasing the denitrifying efficiency. On the other hand, the results obtained for *Paracoccus* biofilm also seems apparent for the ecological adaptation model proposed by Klausen et al. (2006).

Acknowledgements

References

Akolkar A, Bharambe N, Trivedi S, Desai A. 2008. Statistical optimization of medium components for extracellular protease production by an extreme haloarchaeon, *Halobacterium* sp. SP1(1). Lett Appl Microbiol 48:77–83.

APHA. 1995. Standard methods for examination of water and wastewater. 19th edn. Washington, DC: American Public Health Association.

Baker CS, Ferguson SJ, Ludwig B, Page MD, Richter O-MH, Van Spanning RJM. 1998. Molecular genetics of the genus *Paracoccus*: metabolically versatile bacteria with bioenergetic flexibility. Microbiol Mol Bio Rev 62:1046–1078.

Banin E, Vasil ML, Greenberg EP. 2005. Iron and *Pseudomonas aeruginosa* biofilm formation. Proc Natl Acad Sci USA 102:11076–11081.

Banin E, Brady KM, Greenberg EP. 2006. Chelator-induced dispersal and killing of *Pseudomonas aeruginosa* cells in a biofilm. Appl Environ Microbiol 72:2064–2069.

Barraud N, Hassett DJ, Hwang S-H, Rice SA, Kjelleberg S, Webb JS. 2006. Involvement of nitric oxide in biofilm dispersal of *Pseudomonas aeruginosa*. J Bacteriol 188:7344–7353.

Boles RB, Thoendel M, Singh PK. 2004. Self generated diversity produces "insurance effects" in biofilm communities. Proc Natl Acad Sci USA 101:16630–16635.

Chen X, Stewart PS. 2002. Role of electrostatic interactions in cohesion of bacterial biofilms. Appl Microbiol Biotechnol 59:718–720.

Costerton JW, Lewandowski Z, Caldwell DE, Korber DR, Lappin-Scott HM. 1995. Microbial biofilms. Annu Rev Microbiol 49:711–745.

Deighton M, Borland R. 1993. Regulation of slime production in *Staphylococcus epidermidis* by iron limitation. Infect Immun 61:4473–4479.

Dunne WM, Burd EM. 1992. The effects of magnesium, calcium, EDTA and pH on the *in vitro* adhesion of *Staphylococcus epidermidis* to plastic. Microbiol Immun 36:1019–1027.

Garcia-Godoy F, Hicks MJ. 2008. Maintaining the integrity of the enamel surface: the role of dental biofilm, saliva and preventive agents in enamel demineralization and remineralization. J Am Dent Assoc 139:25S–34S.

Geesey GG, Wigglesworth-Cooksey B, Cooksey KE. 2000. Influence of calcium and other cations on surface adhesion of bacteria and diatoms: a review. Biofouling 15:195–205.

Gohel V, Chaudhary T, Vyas P, Chhatpar HS. 2006. Statistical screenings of medium components for the production of chitinase by the marine isolate *Pantoea dispersa*. Biochem Eng J 28:50–56.

Hall-Stoodley L, Costerton JW, Stoodley P. 2004. Bacterial biofilms: from the natural environment to infectious diseases. Nat Rev Microbiol 2:95–108.

Heydorn A, Nielsen AT, Hentzer M, Sternberg C, Givskov M, Ersboll BK, Molin S. 2000. Quantification of biofilm structures by the novel computer program COMSTAT. Microbiology 146:2395–2407.

Jenkins D, Medsker LL. 1964. Brucine method for determination of nitrate in ocean, estuarine and fresh waters. Anal Chem 36:610–612.

Johnson M, Cockayne A, Williams PH, Morrissey JA. 2005. Iron-responsive regulation of biofilm formation in *Staphylococcus aureus* involves Fur-dependent and Fur-independent mechanisms. J Bacteriol 187:8211–8215.

Kierek K, Watnick PI. 2003. The *Vibrio cholerae* O139 O-antigen polysaccharide is essential for Ca^{2+}-dependent biofilm development in sea water. Proc Natl Acad Sci USA 100:14357–14362.

Klausen M, Gjermansen M, Kreft JU, Tolker-Nielsen T. 2006. Dynamics of development and dispersal in sessile microbial communities: examples from *Pseudomonas aeruginosa* and *Pseudomonas putida* model biofilms. FEMS Microbiol Lett 261:1–11.

Lattner D, Flemming HC, Mayer C. 2003. ^{13}C-NMR study of the interaction of bacterial alginate with bivalent cations. Int J Biol Macromol 33:81–88.

Lowry OH, Rosebrough NJ, Farr AL, Randall RJ. 1951. Protein measurement with the Folin phenol reagent. J Biol Chem 193:265–275.

Moller S, Korber DR, Wolfaard GM, Molin S, Caldwell DE. 1997. Impact of nutrient composition on a degradative biofilm community. Appl Environ Microbiol 63: 2432–2438.

Monds RD, Newell PD, Gross RH, O'Toole GA. 2007. Phosphate-dependent modulation of c-di-GMP levels regulates *Pseudomonas fluorescens* Pf0-1 biofilm formation by controlling secretion of the adhesin LapA. Mol Microbiol 63:656–679.

Montgomery DC. 1997. Design and analysis of experiments. 4th edn. New York: Wiley.

Moorthy S, Watnick PI. 2004. Genetic evidence that the *Vibrio cholerae* monolayer is a distinct stage in biofilm development. Mol Microbiol 52:573–587.

Musk DJ, Banko DA, Hergenrother PJ. 2005. Iron salts perturb biofilm formation and disrupt existing biofilms of *Pseudomonas aeruginosa*. Chem Biol 12:789–796.

O'Toole G, Kaplan HB, Kolter R. 2000. Biofilm formation as microbial development. Annu Rev Microbiol 54:49–79.

Peng X, Zhang JS, Li YY, Li W, Xu GM, Yan CY. 2008. Biodegradation of insecticide carbofuran by *Paracoccus* sp. YM3. J Environ Sci Health Part B 43:588–594.

Plackett RL, Burman JP. 1946. The design of optimum multifactorial experiments. Biometrika 33:305–325.

Prakash B, Veeregowda BM, Krishnappa G. 2003. Biofilms: a survival strategy of bacteria. Curr Sci 85:1299–1307.

Priester JH, Horst AM, Werfhorst LCVD, Saleta JL, Mertes LAK, Holden PA. 2007. Enhanced visualization of microbial biofilms by staining and environmental scanning electron microscopy. J Microbiol Methods 68: 577–587.

Rose RK. 2000. The role of calcium in oral streptococcal aggregation and the implications for biofilm formation and retention. Biochim Biophys Acta 1475:76–82.

Sarsikova S, Patrauchan MA, Berglund D, Nivens DE, Franklin MJ. 2005. Calcium-induced virulence factors associated with the extracellular matrix of mucoid *Pseudomonas aeruginosa* biofilms. J Bacteriol 187:4327–4337.

Sauer K, Cullen MC, Rickard AH, Zeef LAH, Davies DG, Gilbert P. 2004. Characterization of nutrient-induced dispersion in *Pseudomonas aeruginosa* PAO1 biofilm. J Bacteriol 186:7312–7326.

Schlag S, Nerz C, Birkenstock TA, Altenberend F, Go"tz F. 2007. Inhibition of staphylococcal biofilm formation by nitrite. J Bacteriol 189:7911–7919.

Siller H, Rainey FA, Stackebrandt E, Winter J. 1996. Isolation and characterization of a new Gram-negative, acetone-degrading, nitrate-reducing bacterium from soil, *Paracoccus solventivorans* sp. nov. Int J Syst Evol Microbiol 46:1125–1130.

Singh PK, Parsek MR, Greenberg EP, Welsh MJ. 2002. A component of innate immunity prevents bacterial biofilm development. Nature 417:552–555.

Song B, Leff LG. 2006. Influence of magnesium ions on biofilm formation by *Pseudomonas fluorescens*. Microbiol Res 161:355–361.

Srinivas MRS, Chand N, Lonsane BK. 1994. Use of Plackett-Burman design for rapid screening of several nitrogen sources, growth/product promoters, minerals and enzyme inducers for the production of alpha-galactosidase by *Aspergillus niger* MRSS 234 in solid state fermentation system. Biopro Biosys Eng 10: 1615–7591.

Stoodley P, Sauer K, Davies DG, Costerton JW. 2002. Biofilms as complex differentiated communities. Annu Rev Microbiol 56:187–209.

Sutherland I. 2001. Biofilm exopolysaccharides: a strong and sticky framework. Microbiology 147:3–9.

Tanji Y, Morono Y, Soejima A, Hori K, Unno H. 1999. Structural analysis of a biofilm which enhances carbon steel corrosion in nutritionally poor aquatic environments. J Biosci Bioeng 88:551–556.

Tiedje JM. 1994. Denitrifiers. In: Weaver RW, Angle JS, Bottomley PS, editors. Methods of soil analysis. Part 2. Microbiological and biochemical properties. Madison, Wisconsin: Soil Science Society of America. p. 245–267.

Turakhia MH, Cooksey KE, Characklis WG. 1983. Influence of a calcium-specific chelant on biofilm removal. Appl Environ Microbiol 46:1236–1238.

Urakami T, Hisaya A, Hiromi O, Ken-Ichiro S, Kazuo K. 1990. *Paracoccus aminophilus* sp. nov. and *Paracoccus aminovorans* sp. nov. which utilize N, N-dimethylformamide. Int J Syst Evol Microbiol 40:287–291.

Vasilyeva GK, Bakhaeva LP, Strijakova ER, Patrick JS. 2003. Bioremediation of 3,4-dichloroaniline and 2,4,6-trinitrotoluene in soil in the presence of natural adsorbents. Environ Chem Lett 1:179–183.

Vlamikis H, Aguilar C, Losick R, Kolter R. 2008. Control of cell fate by the formation of an architecturally complex bacterial community. Genes Dev 22:945–953.

Watnick P, Kolter R. 2000. Biofilm, city of microbes. J Bacteriol 182:2675–2679.

Wimpenny JWT, Colasanti R. 1997. A unifying hypothesis for the structure of microbial biofilms based on cellular automaton models. FEMS Microbiol Ecol 22:1–16.

Xu G, Zheng W, Li Y, Wang S, Zhang J, Yan Y. 2008. Biodegradation of chlorpyrifos and 3,5,6-trichloro-2-pyridinol by a newly isolated *Paracoccus* sp. strain TRP. Int Biodeterior Biodegr 62:51–56.

Yang L, Barken KB, Skindersoe ME, Christensen AB, Givskov M, Tolker-Nielsen T. 2007. Effects of iron on DNA release and biofilm development by *Pseudomonas aeruginosa*. Microbiology 153:1318–1328.

Comparison of Denitrification Between *Paracoccus* sp. and *Diaphorobacter* sp.

Srinandan S. Chakravarthy • Samay Pande •
Ashish Kapoor • Anuradha S. Nerurkar

Abstract Denitrification was compared between *Paracoccus* sp. and *Diaphorobacter* sp. in this study, both of which were isolated from activated sludge of a denitrifying reactor. Denitrification of both isolates showed contrasting patterns, where *Diaphorobacter* sp. showed accumulation of nitrite in the medium while *Paracoccus* sp. showed no accumulation. The nitrate reduction rate was 1.5 times more than the nitrite reduction in *Diaphorobacter* sp., as analyzed by the resting state denitrification kinetics. Increasing the nitrate concentration in the medium increased the nitrite accumulation in *Diaphorobacter* sp., but not in *Paracoccus* sp., indicating a branched electron transfer during denitrification. *Diaphorobacter* sp. was unable to denitrify efficiently at high nitrate concentrations from 1 M, but *Paracoccus* sp. could denitrify even up to 2 M nitrate. *Paracoccus* sp. was found to be an efficient denitrifier with insignificant amounts of nitrite accumulation, and it could also denitrify high amounts of nitrate up to 2 M. Efficient denitrification without accumulation of intermediates like nitrite is desirable in the removal of high nitrates from wastewaters. *Paracoccus* sp. is shown to suffice this demand and could be a potential organism to remove high nitrates effectively.

Keywords Denitrification · Wastewater treatment · *Paracoccus* sp. · *Diaphorobacter* sp. · High nitrate removal

Introduction

Denitrification is the bacterial respiratory process that couples electron transport phosphorylation with sequential reduction of nitrate to nitrogen through the intermediates nitrite, nitric oxide, and nitrous oxide [34]. The denitrifying ability of bacteria is widely distributed among several genera, though the frequency is more among the alpha and beta proteobacteria [35]. However, the reduction rate of nitrogenous oxides during the

S. S. Chakravarthy • S. Pande • A. Kapoor • A. S. Nerurkar (✉)
Department of Microbiology and Biotechnology Centre, Faculty of Science,
The M. S. University of Baroda, Vadodara, Gujarat, India
e-mail: anuner26@yahoo.com

⚐ Springer

denitrification process varies in different species and even strains [4, 5]. Environmental factors are known to significantly affect the denitrification process [12, 28, 29]. Partial pressure of oxygen is reported to determine the synthesis of reductases differentially, and nitrate is also known to affect nitrite reduction in *Pseudomonas stutzeri* [17]. Almeida et al. [2] observed the dependency of nitrite reduction on the nitrate concentrations in *Pseudomonas flourescens*. Low nitrite than nitrate reduction causes the buildup of nitrite, and the accumulated nitrite limits denitrification and growth [1]. Almeida et al. [2] showed that nitrite concentrations above 130 mg NL^{-1} limit the growth of *P. flourescens*.

Wastewaters of certain industries producing chemicals, fertilizers, explosives, etc., contain very high amounts of nitrate with more than 1,000 mg L^{-1} [7, 10, 13, 33], which, when released into the environment such as lakes or rivers, causes eutrophication and also contaminates the drinking water. The WHO guideline values for nitrate and nitrite in drinking water are 50 and 3 mg L^{-1}, respectively [31], because consumption of high nitrate and nitrite concentrations are known to cause methemoglobinemia in infants and other health hazards. Biological denitrification is the widely used phenomenon for nitrate removal from wastewaters. However, prominent limiting conditions for efficient denitrification to occur in reactors are high nitrate concentrations in wastewaters [6, 8, 11] and the accumulation of nitrite [12, 26]. Francis and Mankin [11] observed nitrate concentrations above 6 kg L^{-1} to inhibit nitrate reduction. High nitrate concentrations possibly limit denitrification because of their chaotropic effect and also because the denitrification intermediates, nitrite and nitric oxide, generate reactive nitrogen species (RNS) which are harmful to cells [25].

Thus, denitrifiers which can reduce high nitrate concentration without accumulation of intermediates are a necessity in denitrifying reactors to increase the process efficiency. In order to check the denitrification potential of the bacteria present in denitrifying reactors, we isolated two cultures and compared their denitrification patterns at different nitrate concentrations. The cultures under study were *Paracoccus* sp. W1b (henceforth *Paracoccus*) and *Diaphorobacter* sp. D1 (henceforth *Diaphorobacter*), both isolated from activated sludge of a denitrifying reactor. Different strains of both cultures are known to thrive in sludge habitats [15, 20, 21, 32]. Our study shows that *Paracoccus* could denitrify more efficiently and also tolerate high nitrate concentrations than *Diaphorobacter*.

Materials and Methods

Isolation and Identification of Bacteria

Isolates W1b and D1 were isolated from the denitrifying reactor sludge of a fertilizer factory on peptone nitrate agar plates. Identification of the isolates was done by sequencing the partial 16S rRNA gene. The primers used for amplifying 16S rRNA gene by PCR were 27f (5'-GAGAGTTTGATCTGGCTCAG-3') and 1541r (5'-AAGGAGGTGATCCAGCCG-3'). Sequencing of the PCR amplicon was done in ABI *3730xl* DNA Analyzer at services provided by XcelrisLabs. The primers used for sequencing the PCR product were 27f, 1541r, and also 341f (5'-CTACGGGAGGCAGCA-3'), 534r (5'-ATTACCGCGGCTGCTGG-3'), and 1107r (5'-GCTCGTTGCGGGACTTAA-3') according to Pillai and Archana [23]. Overlapping sequences were analyzed in Mega 4.1 software [19] and corrected to obtain a larger fragment of the 16S rRNA gene. The sequences are submitted to the NCBI data bank with accession numbers HQ625227 and HQ625228.

Culture Conditions

Culture maintenance and inoculum preparation was done in peptone nitrate medium (PNB). Denitrification experiments were performed in MM2 medium [27] consisting of sodium succinate 7.9 g, $MgSO_4 \cdot 7H_2O$ 0.2 g, K_2HPO_4 0.2 g, $FeSO_4 \cdot 7H_2O$ 0.05 g, $CaCl_2 \cdot 2H_2O$ 0.02 g, $MnCl_2 \cdot 4H_2O$ 0.002 g, $NaMoO_4 \cdot 2H_2O$ 0.001 g, KNO_3 1.0 g, yeast extract 1.0 g, pH 7.0, and distilled water 1,000 mL. A 24-h-old culture was centrifuged, washed, and resuspended in phosphate-buffered saline (PBS) for inoculation in denitrification experiments. Incubation of the cultures was done at 30 °C in static conditions for maintenance of anoxia.

Denitrification Studies

Denitrification during growth was monitored up to 36 h with nitrate and nitrite measured in intervals of 6 h. The experiment was performed in 250-mL Erlenmeyer flasks in MM2 medium containing 10 mM KNO_3 inoculated with 10^8 cells mL^{-1} of a 24-h-old culture.

Nitrate reduction, nitrite formation, and the relative rates (RR) of nitrate and nitrite reduction were calculated according to Dhamole et al. [9], where relative rate is described as

$$RR = \frac{K_{NO3}}{K_{NO3} - k_{NO2}}$$

where K_{NO3} is the rate of nitrate reduction and k_{NO2} is the rate of nitrite formation in the presence of nitrate.

Nitrate and nitrite reduction rates by resting cell suspension were performed as follows: Cells grown for 24 h in peptone nitrate broth were harvested by centrifugation at 10,000 rpm for 5 min, washed twice with phosphate-buffered saline (pH 7.4), and resuspended in PBS. Succinate and nitrate were added as electron donor and acceptor, respectively, and the reductions of nitrate and nitrite were estimated for 20 min.

Denitrification experiments at high nitrates were done in 24-well microtiter plates using 3 mL MM2 medium with the C/N ratio of 5.0 maintained at appropriate nitrate concentration. High nitrate concentrations were used in this experiment from 0.1 to 2 M. About 10^8 cells mL^{-1} were used as inoculum and incubated for 12 h, after which colony-forming units (CFU), nitrate, and nitrite were measured.

Analytical Methods

Nitrate was estimated according to the method described by Jenkins and Medsker [14]. Nitrite was determined according to the standard method described in APHA [3]. The method of Lowry et al. [22] was used for protein estimation, with bovine serum albumin as a standard.

Production of nitrous oxide by the culture was analyzed by withdrawing the sample from the headspace of the test tube in which the isolate was grown for 18 h in PNB medium, and N_2O was measured by gas chromatography (Perkin Elmer, Auto system XL) with an electron capture detector.

Results

Characterization of the Isolates

The two cultures under study, W1b and D1, were isolated from the denitrifying reactor sludge sample of a fertilizer industry in peptone nitrate medium. The presence of nitrous oxide in the headspace of the growth tube confirmed them to be denitrifiers. Isolate W1b was observed to be a Gram-negative cocci, and BLAST results of 1,094-bp partial 16S rRNA gene showed 99% identity with *Paracoccus* species; isolate D1, a Gram-negative rod, showed 98% similarity with *Diaphorobacter* species with a 1,437-bp partial 16S rRNA gene sequence. Phylogenetic positions of both the isolates are shown in Fig. 1, where the isolates W1b and D1 clustered with *Paracoccus* sp. and *Diaphorobacter* sp., respectively.

Denitrification Pattern of the Isolates

The nitrate reduction and nitrite accumulation of both isolates were monitored in batch mode up to 36 h in 250-mL Erlenmeyer flasks under static condition. Nitrate was reduced to 1.65 mM from 12.0 mM in 36 h by *Paracoccus*, with insignificant amount of nitrite accumulation at the 6-h interval (Fig. 2). *Diaphorobacter* could reduce nitrate from 12.0 to
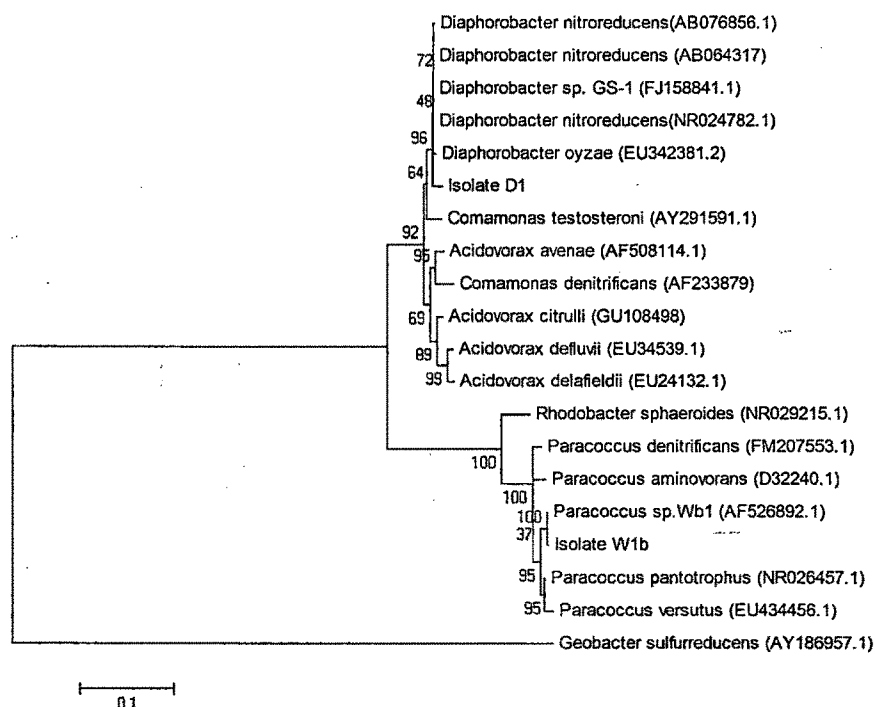
Fig. 1 Phylogenetic tree constructed by neighbor-joining method showing position of the isolates with other related cultures. Bootstrap analysis of 1,000 resampling by maximum-likelihood method was used to construct tree. *Parenthesis* contains the accession number of the cultures
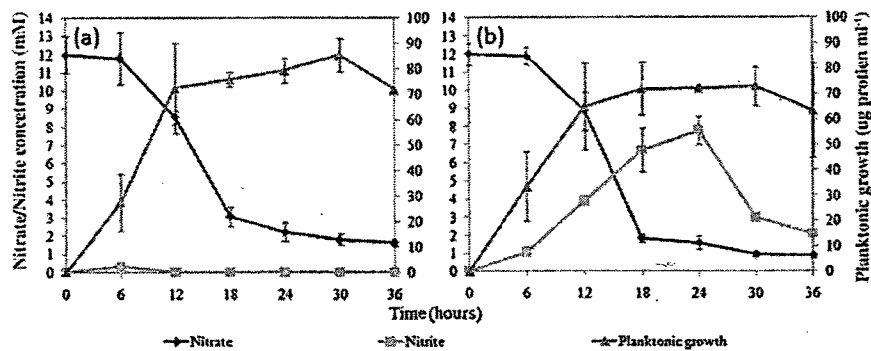
Fig. 2 Denitrification pattern of the isolates (a) *Paracoccus* and (b) *Diaphorobacter.* Error bars represent the standard deviation

0.89 mM in 36 h, whereas a substantial amount of nitrite was accumulated in the medium (Fig. 2). Accumulation of nitrite increased to around 7.8 mM in 24 h and decreased to 2.1 mM at 36 h. The calculated RR was high in *Diaphorobacter* and nearly 1.14 in *Paracoccus* (Table 1), suggesting that the rate differences between nitrate and nitrite reduction is the possible reason for nitrite accumulation.

The reduction rates of nitrogenous oxides were further estimated in the resting state of these cultures. The nitrate reduction rate was 1.5-fold higher than the nitrite reduction rate in *Diaphorobacter*, whereas the nitrate to nitrite reduction rate ratio of *Paracoccus* was found to be 1.0 (Table 2), suggesting similar reduction rates of nitrate and nitrite. However, the influence of increasing nitrate concentrations on the reduction of nitrite showed an increased accumulation of nitrite in *Diaphorobacter*, whereas nitrite buildup was not observed in *Paracoccus* with the increase in nitrate concentration (Fig. 3). The nitrate reduction rate at increasing nitrate concentrations is shown in Table 3, where the nitrate reduction rate increased substantially with 10 mM nitrate.

Influence of C/N Ratio on Denitrification by the Isolates

The amount of carbon source plays a crucial role in reducing nitrates in denitrifying reactors, so the optimum C/N ratio was tested for efficient denitrification in the cultures. Nitrate was provided as both electron acceptor and nitrogen source in the medium to the bacteria. Growth and nitrate reductions were significantly affected in both the isolates at a C/N ratio of <1, but much differences were not found at increasing C/N ratios more than 1.0 (Fig. 4a, d). An increase in nitrite accumulation was seen at decreasing C/N ratio in

Table 1 Calculated rates during denitrification deduced from data shown in Fig. 2

Isolates	NO_3 reduction (μM min^{-1})	NO_2 formation (μM min^{-1})	RR
Paracoccus sp.	7.22	0.9	1.14
Diaphorobacter sp.	9.72	6.1	2.68

Rates were calculated according to Dhamole et al. [9]. RR = 1 implies no nitrite buildup, whereas RR > 1 signifies nitrite accumulation

RR relative rate of nitrate and nitrite reduction

Rates determined by linear regression. R^2 >0.87

Table 2 Nitrate and nitrite reduction rates by resting-state cells

| Isolates	NO$_3$ reduced (µM mg^{-1} protein min^{-1})	NO$_2$ reduced (µM mg^{-1} protein min^{-1})	Ratio of nitrate to nitrite reduction
Paracoccus sp.	159.0±85.0	147.0±15.0	1.08
Diaphorobacter sp.	117.0±13.0	78.0±14.0	1.50

Paracoccus, though significant nitrite accumulation changes were not observed in *Diaphorobacter* with changes in the C/N ratio (Fig. 4b, e). A 27-fold increase in nitrite was seen in a C/N ratio of 0.25 than 1.0, and a C/N ratio of 0.5 showed a 9-fold increase in nitrite than the C/N ratio of 1.0 in *Paracoccus* (Fig. 4b). Nitrite accumulation was in the range of 3.5–6.9 mM in *Diaphorobacter* at all C/N ratios (Fig. 4e).

High Nitrate Denitrification by the Isolates

Nitrate reduction and accumulation of nitrite was investigated in both the isolates at high nitrate concentrations, the results of which are shown in Table 4. A C/N ratio of 5.0 was maintained at all nitrate concentrations tested. *Paracoccus* reduced nitrate in the range 54–76.5% in 12 h for all the nitrate concentrations tested. Nitrite accumulation was in the range 1.15–3.4 mM, although 6.5 mM nitrite accumulated with 0.5 M initial nitrate. An average CFU of 10^9 mL^{-1} was maintained at all tested nitrate concentrations (Table 4). Nitrate reduction was high in *Diaphorobacter* in the range 70–80% up to 0.5 M initial nitrate concentration, whereas a drastic decrease in nitrate reduction with 17.5% and 15.7% and a 2 log decrease in CFU with 10^7 cells were observed when nitrate was increased to 1 and 2 M, respectively. Nitrite accumulation in *Diaphorobacter* was higher than *Paracoccus*, with a range of 8.1–13.6 mM.

Discussion

Though similar denitrification apparatus is present in diverse groups of bacteria, the denitrifying activity of each step differs in different organisms. In this study, we compared
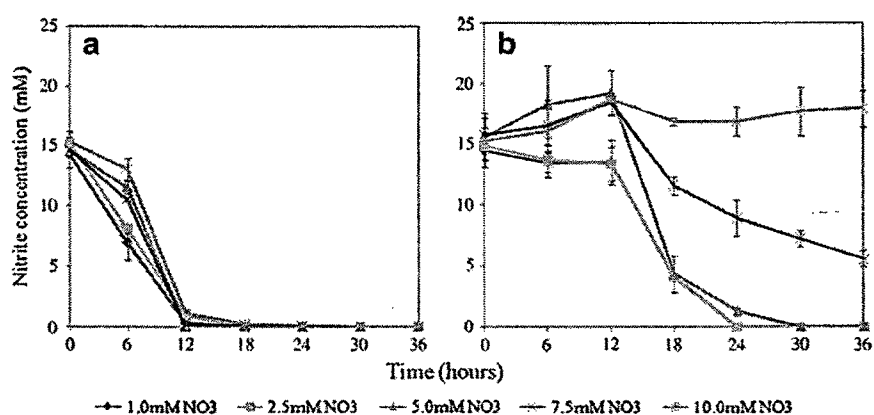
Fig. 3 Nitrite accumulation at increasing nitrate concentrations in the medium. a *Paracoccus*, b *Diaphorobacter*. Error bars represent the standard deviation

Table 3 Nitrate reduction rates during denitrification at increasing nitrate concentrations	Initial nitrate concentration (mM)	Nitrate reduction (μM min^{-1})	
		Paracoccus	Diaphorobacter
	1.0	3.08	5.25
	2.5	4.16	5.00
	5.0	4.16	4.16
	7.5	5.27	5.27
Rates determined by linear regression. $R^2 > 0.87$	10.0	8.88	9.44

the denitrification pattern of two cultures, W1b and D1, isolated from the activated sludge of a denitrifying reactor and identified as *Paracoccus* and *Diaphorobacter*, respectively (Fig. 1). The nitrate reduction rate is higher in *Diaphorobacter*, but *Paracoccus* reduced nitrate without much accumulation of nitrite transiently, unlike *Diaphorobacter* which accumulated nitrite significantly (Fig. 2). *Diaphorobacter* species are reported to also nitrify ammonia to nitrite [16]; however, ammonia was not provided in the MM2 medium (refer to "Materials and Methods" for composition), suggesting that the nitrite accumulation was due to nitrate reduction.

Accumulation of nitrogenous oxide intermediates during denitrification was explained by Betlach and Tiedje [4] where they showed that nitrite accumulation in *Alcaligenes* sp. and *P. flourescens* was due to the differences in the reduction rates of nitrate and nitrite. Investigating nitrate and nitrite reduction rates in resting cell suspensions provides insight into the overall reduction rate, including the flux of nitrate/nitrite into and outside the cell. It was observed that *Paracoccus* have a nitrate-to-nitrite reduction ratio of 1.08, suggesting nearly equal rates in the reduction of these two nitrogenous oxides, but *Diaphorobacter* showed a ratio of 1.5 (Table 2). High nitrate than nitrite reduction rate was the possible reason for the accumulation of nitrite in *Diaphorobacter*. Increasing nitrate concentrations
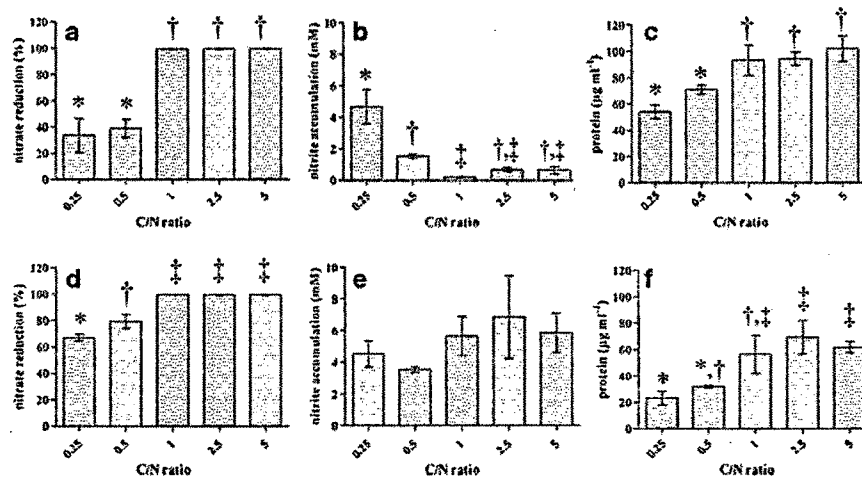
Fig. 4 Influence of the C/N ratio on nitrate reduction, nitrite accumulation, and growth of *Paracoccus* (a–c) and *Diaphorobacter* (d–f). Bars represent the average values of at least three independent experiments. Error bars represent the standard deviation. Same symbols above the bars indicate no significant difference. One-way ANOVA with Tukey test was used to determine significant differences ($p<0.05$)

Table 4 Denitrification and growth of the isolates at high nitrate concentrations

Nitrate concentration (M)					Nitrite accumulation (mM)		CFU[a] ($\times 10^8$)	
Initial	Paracoccus		Diaphorobacter		Paracoccus	Diaphorobacter	Paracoccus	Diaphorobacter
	Final	% reduced	Final	% reduced				
0.1	0.046±0.004	54.0	0.029±0.002	71.0	1.55±0.40	11.3±1.55	10.0	30.0
0.2	0.047±0.0005	76.5	0.040±0.003	80.0	1.15±0.15	13.6±1.45	10.0	50.0
0.5	0.198±0.003	60.4	0.150±0.002	70.0	6.50±2.15	11.8±0.85	10.0	27.0
1.0	0.404±0.077	59.6	0.825±0.246	17.5	2.00±0.45	8.1±4.1	15.0	0.30
2.0	0.693±0.127	65.3	1.686±0.332	15.7	3.40±0.20	9.05±2.05	13.5	0.56

[a] Initial CFU=10^8

in the medium increased the nitrite buildup in *Diaphorobacter*, whereas nitrite accumulation was not observed in *Paracoccus* (Fig. 3). The lower nitrite than nitrate reduction could be the possible reason for the nitrite buildup in *Diaphorobacter*, but a ratio of 1.08 (Table 2) for nitrate to nitrite reduction found in *Paracoccus* could not explain the increased reduction rate of nitrite when nitrate concentrations were increased in the medium. Branched electron flow to the nitrogenous oxides in *Paracoccus denitrificans* has been reported by Kucera et al. [18]. Similarly, the increased nitrite reduction with the increase in nitrate concentration observed for *Paracoccus* (Fig. 3) suggests "inhibition by product via respiratory chain" [18] to be the possible phenomenon.

The C/N ratio significantly influenced nitrate reduction and growth in both the isolates (Fig. 4). Low C/N ratio also affected nitrite accumulation significantly in *Paracoccus*. Carbon source acts as an electron donor; hence, higher amounts of carbon source than nitrate is required to completely reduce nitrates. A C/N ratio of 5.0 was provided in further studies of high nitrate reduction. High nitrate concentrations tested did not affect the nitrate reduction and growth significantly in *Paracoccus*, but a substantial drop in nitrate reduction and growth was observed in *Diaphorobacter* from 1.0 M nitrate concentration (Table 4). Nitrates in excess can be harmful to the cell because of their chaotropic effect. A *Klebsiella oxytoca* strain was isolated by Pinar et al. [24], which could tolerate nitrate up to 1.0 M, but *Klebsiella* species are also reported to have the property of dissimilatory nitrate reduction to ammonium [30]. However, *Paracoccus* could denitrify efficiently even at 2.0 M nitrate concentration and tolerate up to 4.0 M nitrate concentrations (data not shown). The denitrification intermediates, nitrite and nitric oxide, generate RNS which are more toxic to the cells [25]. Efficient denitrification by branched electron transfer [18] in *Paracoccus* is possibly the mechanism to detoxify its microenvironment, whereas the accumulation of nitrite in *Diaphorobacter* possibly lowered the fitness of the cell at high nitrate concentrations.

The above results suggest that *Diaphorobacter* possibly transfers electron sequentially in the denitrification system from nitrate to dinitrogen formation, whereas a branched electron transfer occurs in *Paracoccus*. The branched electron transfer strategy of *Paracoccus* might help the organism adapt to environments containing high nitrogenous oxide concentrations like industrial wastewaters. We have also reported studies on biofilm formation by *Paracoccus* elsewhere [27], and our unpublished data on biofilm community analysis by fluorescence in situ hybridization probes show an increase of *Paracoccus* sp. in the biofilm community at nitrate concentrations above 250 mM in a 1-L laboratory reactor. Efficient denitrification complemented with surface colonization by biofilm formation gives this isolate potential in high nitrate removal processes in denitrifying reactors.

References

1. Almeida, J. S., Julio, S. M., Reis, M. A. M., & Carrondo, M. J. T. (1995). *Biotechnology and Bioengineering, 46*, 194–201.
2. Almeida, J. S., Reis, M. A. M., & Carrondo, M. J. T. (1995). *Biotechnology and Bioengineering, 46*, 476–484.
3. APHA. (1995). *Standard methods* (19th ed.). Washington: American Public Health Association.
4. Betlach, M. R., & Tiedje, J. M. (1981). *Applied and Environmental Microbiology, 42*, 1074–1084.

5. Carlson, C. A., & Ingraham, J. L. (1983). *Applied and Environmental Microbiology, 45*, 1247–1253.
6. Clarkson, W. W., Ross, B. J. B., Krishnamachari, S. (1991). In 45th Purdue Industrial Waste conference Proceedings Lewis Publishers, Inc., Chelsea, MI.
7. Constantin, H., & Fick, M. (1997). *Water Research, 31*, 583–589.
8. Dhamole, P. B., Nair, R. R., D'Souza, S. F., & Lele, S. S. (2007). *Bioresource Technology, 98*, 247–252.
9. Dhamole, P. B., Nair, R. R., D'Souza, S. F., & Lele, S. S. (2008). *Applied Biochemistry and Biotechnology, 151*, 433–440.
10. Fernandez-Nava, Y., Maranon, E., Soons, J., & Castrillon, L. (2008). *Bioresource Technology, 99*, 7976–7981.
11. Francis, C. W., & Mankin, J. B. (1977). *Water Research, 11*, 289–294.
12. Glass, C., & Silverstein, J. (1998). *Water Research, 32*, 831–839.
13. Glass, C., & Silverstein, J. (1999). *Water Research, 33*, 223–229.
14. Jenkins, D., & Medsker, L. L. (1964). *Analytical Chemistry, 36*, 610–612.
15. Khan, S. T., & Hiraishi, A. (2002). *The Journal of General and Applied Microbiology, 48*, 299–308.
16. Khardenavis, A. A., Kapley, A., & Purohit, H. J. (2007). *Applied Microbiology and Biotechnology, 77*, 403–409.
17. Korner, H., & Zumft, W. G. (1989). *Applied and Environmental Microbiology, 55*, 1670–1676.
18. Kucera, I., Dadak, V., & Dobry, R. (1983). *European Journal of Biochemistry. 130*, 359–364.
19. Kumar, S., Nei, M., Dudley, J., & Tamura, K. (2008). *Briefings in Bioinformatics, 9*, 299–306.
20. Lee, M., Woo, S. G., & Kim, M. K. (2011). International Journal of Systematic and Evolutionary Microbiology. doi:10.1099/ijs.0.017897-0.
21. Liu, X.-Y., Wang, B.-J., Jiang, C.-Y., & Liu, S.-J. (2006). *International Journal of Systematic and Evolutionary Microbiology, 56*, 2693–2695.
22. Lowry, O. H., Rosebrough, N. J., Farr, A. L., & Randall, R. J. (1951). *The Journal of Biological Chemistry, 193*, 265–275.
23. Pillai, P., & Archana, G. (2008). *Applied Microbiology and Biotechnology, 78*, 643–650.
24. Pinar, G., Duque, E., Haidour, A., Oliva, J.-M., Sanchez-Barbero, L., Calvo, V., et al. (1997). *Applied and Environmental Microbiology, 63*, 2071–2073.
25. Poole, R. K. (2005). *Biochemical Society Transactions, 33*, 176–180.
26. Rijn, J. V., Tal, Y., & Barak, Y. (1996). *Applied and Environmental Microbiology, 62*, 2615–2620.
27. Srinandan, C. S., Jadav, V., Cecilia, D., & Nerurkar, A. S. (2010). *Biofouling, 26*, 449–459.
28. Thomsen, J. K., Geest, T., & Cox, R. P. (1994). *Applied and Environmental Microbiology, 60*, 536–541.
29. Tiedje, J. M. (1994). In Methods of soil analysis, part 2. Microbiological and biochemical properties. Madison: Soil Science Society of America, pp. 245–267.
30. Tiedje, J. M., Sextone, A. J., Myrold, D. D., & Robinson, J. A. (1982). *Antonie van Leeuwenhoek, 48*, 569–583.
31. WHO (1998). In Guidelines for drinking-water quality, 2nd ed. Addendum to vol. 2, Geneva.
32. Yufei, T., & Guodong, J. (2010). *Bioresource Technology, 101*, 174–180.
33. Zala, S., Nerurkar, A., Desai, A., Ayyer, J., & Akolkar, V. (1999). *Biotechnology Letters, 21*, 481–485.
34. Zumft, W. G. (1992). In A. Ballows, H. G. Triper, M. Dworkin, & W. Harder (Eds.), *The Prokaryotes, I* (pp. 554–581). New York: Springer.
35. Zumft, W. G. (1997). *Microbiology and Molecular Biology Reviews, 61*, 533–616.